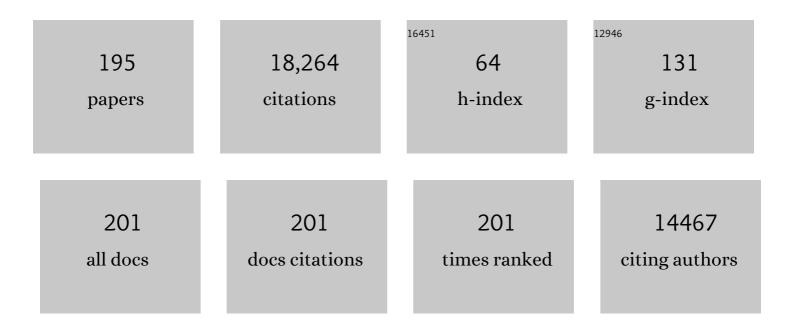
List of Publications by Year in descending order

Source: https://exaly.com/author-pdf/978676/publications.pdf Version: 2024-02-01



EVELYN N MANC

#	Article	IF	CITATIONS
1	Water harvesting from air with metal-organic frameworks powered by natural sunlight. Science, 2017, 356, 430-434.	12.6	1,179
2	Jumping-Droplet-Enhanced Condensation on Scalable Superhydrophobic Nanostructured Surfaces. Nano Letters, 2013, 13, 179-187.	9.1	950
3	A nanophotonic solar thermophotovoltaic device. Nature Nanotechnology, 2014, 9, 126-130.	31.5	704
4	Nanostructured materials for water desalination. Nanotechnology, 2011, 22, 292001.	2.6	543
5	Effect of Droplet Morphology on Growth Dynamics and Heat Transfer during Condensation on Superhydrophobic Nanostructured Surfaces. ACS Nano, 2012, 6, 1776-1785.	14.6	514
6	Uni-directional liquid spreading on asymmetric nanostructured surfaces. Nature Materials, 2010, 9, 413-417.	27.5	473
7	Structured surfaces for enhanced pool boiling heat transfer. Applied Physics Letters, 2012, 100, .	3.3	440
8	Concentrating Solar Power. Chemical Reviews, 2015, 115, 12797-12838.	47.7	438
9	Nanoengineered materials for liquid–vapour phase-change heat transfer. Nature Reviews Materials, 2017, 2, .	48.7	431
10	Adsorption-based atmospheric water harvesting device for arid climates. Nature Communications, 2018, 9, 1191.	12.8	401
11	Wettability of Graphene. Nano Letters, 2013, 13, 1509-1515.	9.1	400
12	Optimization of nanofluid volumetric receivers for solar thermal energy conversion. Solar Energy, 2012, 86, 253-265.	6.1	368
13	Condensation on Superhydrophobic Surfaces: The Role of Local Energy Barriers and Structure Length Scale. Langmuir, 2012, 28, 14424-14432.	3.5	347
14	Condensation heat transfer on superhydrophobic surfaces. MRS Bulletin, 2013, 38, 397-406.	3.5	329
15	Ultrahigh-efficiency desalination <i>via</i> a thermally-localized multistage solar still. Energy and Environmental Science, 2020, 13, 830-839.	30.8	317
16	Methylammonium Bismuth Iodide as a Leadâ€Free, Stable Hybrid Organic–Inorganic Solar Absorber. Chemistry - A European Journal, 2016, 22, 2605-2610.	3.3	312
17	How Coalescing Droplets Jump. ACS Nano, 2014, 8, 10352-10362.	14.6	304
18	High-performance subambient radiative cooling enabled by optically selective and thermally insulating polyethylene aerogel. Science Advances, 2019, 5, eaat9480.	10.3	281

#	Article	IF	CITATIONS
19	Record Atmospheric Fresh Water Capture and Heat Transfer with a Material Operating at the Water Uptake Reversibility Limit. ACS Central Science, 2017, 3, 668-672.	11.3	275
20	Reversible Wettingâ^'Dewetting Transitions on Electrically Tunable Superhydrophobic Nanostructured Surfaces. Langmuir, 2007, 23, 9128-9133.	3.5	251
21	Scalable Graphene Coatings for Enhanced Condensation Heat Transfer. Nano Letters, 2015, 15, 2902-2909.	9.1	236
22	Metallic Photonic Crystal Absorberâ€Emitter for Efficient Spectral Control in Highâ€Temperature Solar Thermophotovoltaics. Advanced Energy Materials, 2014, 4, 1400334.	19.5	230
23	Modeling and Optimization of Superhydrophobic Condensation. Journal of Heat Transfer, 2013, 135, .	2.1	224
24	Immersion Condensation on Oil-Infused Heterogeneous Surfaces for Enhanced Heat Transfer. Scientific Reports, 2013, 3, 1988.	3.3	222
25	Adsorption-Based Atmospheric Water Harvesting: Impact of Material and Component Properties on System-Level Performance. Accounts of Chemical Research, 2019, 52, 1588-1597.	15.6	219
26	Hierarchically structured surfaces for boiling critical heat flux enhancement. Applied Physics Letters, 2013, 102, .	3.3	216
27	Graphene cleans up water. Nature Nanotechnology, 2012, 7, 552-554.	31.5	209
28	Electrostatic charging of jumping droplets. Nature Communications, 2013, 4, 2517.	12.8	201
29	Phase change phenomena in silicon microchannels. International Journal of Heat and Mass Transfer, 2005, 48, 1572-1582.	4.8	189
30	Condensation on Superhydrophobic Copper Oxide Nanostructures. Journal of Heat Transfer, 2013, 135,	2.1	187
31	Electric-Field-Enhanced Condensation on Superhydrophobic Nanostructured Surfaces. ACS Nano, 2013, 7, 11043-11054.	14.6	180
32	Passive directional sub-ambient daytime radiative cooling. Nature Communications, 2018, 9, 5001.	12.8	179
33	Dual-Stage Atmospheric Water Harvesting Device for Scalable Solar-Driven Water Production. Joule, 2021, 5, 166-182.	24.0	173
34	Prediction and Optimization of Liquid Propagation in Micropillar Arrays. Langmuir, 2010, 26, 15070-15075.	3.5	164
35	Jumping-droplet electrostatic energy harvesting. Applied Physics Letters, 2014, 105, .	3.3	163
36	Effect of hydrocarbon adsorption on the wettability of rare earth oxide ceramics. Applied Physics Letters, 2014, 105, .	3.3	154

#	Article	IF	CITATIONS
37	Nanoporous membrane device for ultra high heat flux thermal management. Microsystems and Nanoengineering, 2018, 4, 1.	7.0	154
38	Passive, high-efficiency thermally-localized solar desalination. Energy and Environmental Science, 2021, 14, 1771-1793.	30.8	142
39	Design of Lubricant Infused Surfaces. ACS Applied Materials & amp; Interfaces, 2017, 9, 42383-42392.	8.0	131
40	Non-wetting droplets on hot superhydrophilic surfaces. Nature Communications, 2013, 4, 2518.	12.8	129
41	Surface Structure Enhanced Microchannel Flow Boiling. Journal of Heat Transfer, 2016, 138, .	2.1	129
42	Unified Model for Contact Angle Hysteresis on Heterogeneous and Superhydrophobic Surfaces. Langmuir, 2012, 28, 15777-15788.	3.5	127
43	Bubble growth and departure modes on wettable/non-wettable porous foams in alkaline water splitting. Joule, 2021, 5, 887-900.	24.0	123
44	Realâ€īime Manipulation with Magnetically Tunable Structures. Advanced Materials, 2014, 26, 6442-6446.	21.0	120
45	Enabling Ideal Selective Solar Absorption with 2D Metallic Dielectric Photonic Crystals. Advanced Materials, 2014, 26, 8041-8045.	21.0	120
46	Design of micropillar wicks for thin-film evaporation. International Journal of Heat and Mass Transfer, 2016, 101, 280-294.	4.8	116
47	Turning bubbles on and off during boiling using charged surfactants. Nature Communications, 2015, 6, 8599.	12.8	115
48	Heat Transfer Enhancement During Water and Hydrocarbon Condensation on Lubricant Infused Surfaces. Scientific Reports, 2018, 8, 540.	3.3	111
49	Porous Cu Nanowire Aerosponges from One tep Assembly and their Applications in Heat Dissipation. Advanced Materials, 2016, 28, 1413-1419.	21.0	109
50	Thermophotovoltaic efficiency of 40%. Nature, 2022, 604, 287-291.	27.8	108
51	Analytical model for the design of volumetric solar flow receivers. International Journal of Heat and Mass Transfer, 2012, 55, 556-564.	4.8	101
52	Highly efficient and salt rejecting solar evaporation via a wick-free confined water layer. Nature Communications, 2022, 13, 849.	12.8	101
53	Modeling and optimization of hybrid solar thermoelectric systems with thermosyphons. Solar Energy, 2011, 85, 2843-2855.	6.1	100
54	Harnessing Heat Beyond 200 °C from Unconcentrated Sunlight with Nonevacuated Transparent Aerogels. ACS Nano, 2019, 13, 7508-7516.	14.6	97

#	Article	IF	CITATIONS
55	Biotemplated hierarchical surfaces and the role of dual length scales on the repellency of impacting droplets. Applied Physics Letters, 2012, 100, .	3.3	87
56	High-resolution liquid patterns via three-dimensional droplet shape control. Nature Communications, 2014, 5, 4975.	12.8	85
57	Negative pressures in nanoporous membranes for thin film evaporation. Applied Physics Letters, 2013, 102, .	3.3	82
58	Interplay between hydrophilicity and surface barriers on water transport in zeolite membranes. Nature Communications, 2016, 7, 12762.	12.8	80
59	Modeling of Evaporation from Nanopores with Nonequilibrium and Nonlocal Effects. Langmuir, 2015, 31, 9817-9824.	3.5	78
60	Tunable Metal–Organic Frameworks Enable High-Efficiency Cascaded Adsorption Heat Pumps. Journal of the American Chemical Society, 2018, 140, 17591-17596.	13.7	78
61	A Passive High-Temperature High-Pressure Solar Steam Generator for Medical Sterilization. Joule, 2020, 4, 2733-2745.	24.0	76
62	A unified relationship for evaporation kinetics at low Mach numbers. Nature Communications, 2019, 10, 2368.	12.8	73
63	A Hybrid Electric and Thermal Solar Receiver. Joule, 2018, 2, 962-975.	24.0	70
64	Precise control of pore hydrophilicity enabled by post-synthetic cation exchange in metal–organic frameworks. Chemical Science, 2018, 9, 3856-3859.	7.4	70
65	Kinetics of Sorption in Hygroscopic Hydrogels. Nano Letters, 2022, 22, 1100-1107.	9.1	65
66	Thermal Spreading Resistance and Heat Source Temperature in Compound Orthotropic Systems With Interfacial Resistance. IEEE Transactions on Components, Packaging and Manufacturing Technology, 2013, 3, 1826-1841.	2.5	64
67	Thermal battery for portable climate control. Applied Energy, 2015, 149, 104-116.	10.1	63
68	Analytical Solution for Temperature Rise in Complex Multilayer Structures With Discrete Heat Sources. IEEE Transactions on Components, Packaging and Manufacturing Technology, 2014, 4, 817-830.	2.5	62
69	Prediction and Characterization of Dry-out Heat Flux in Micropillar Wick Structures. Langmuir, 2016, 32, 1920-1927.	3.5	62
70	Toward Condensation-Resistant Omniphobic Surfaces. ACS Nano, 2018, 12, 11013-11021.	14.6	62
71	An Ultrathin Nanoporous Membrane Evaporator. Nano Letters, 2017, 17, 6217-6220.	9.1	60
72	Characterization of Adsorption Enthalpy of Novel Water-Stable Zeolites and Metal-Organic Frameworks. Scientific Reports, 2016, 6, 19097.	3.3	59

#	Article	IF	CITATIONS
73	Effects of millimetric geometric features on dropwise condensation under different vapor conditions. International Journal of Heat and Mass Transfer, 2018, 119, 931-938.	4.8	55
74	Optimization of adsorption processes for climate control and thermal energy storage. International Journal of Heat and Mass Transfer, 2014, 77, 288-300.	4.8	54
75	Design and Modeling of Membrane-Based Evaporative Cooling Devices for Thermal Management of High Heat Fluxes. IEEE Transactions on Components, Packaging and Manufacturing Technology, 2016, 6, 1056-1065.	2.5	54
76	Thermal Expansion Coefficient of Monolayer Molybdenum Disulfide Using Micro-Raman Spectroscopy. Nano Letters, 2019, 19, 4745-4751.	9.1	54
77	Design of an Integrated Loop Heat Pipe Air-Cooled Heat Exchanger for High Performance Electronics. IEEE Transactions on Components, Packaging and Manufacturing Technology, 2012, 2, 1637-1648.	2.5	53
78	Effect of Hydrophilic Defects on Water Transport in MFI Zeolites. Langmuir, 2014, 30, 6446-6453.	3.5	53
79	Parametric study of thin film evaporation from nanoporous membranes. Applied Physics Letters, 2017, 111, .	3.3	53
80	High temperature annealing for structural optimization of silica aerogels in solar thermal applications. Journal of Non-Crystalline Solids, 2017, 462, 72-77.	3.1	52
81	Modeling and performance analysis of high-efficiency thermally-localized multistage solar stills. Applied Energy, 2020, 266, 114864.	10.1	52
82	Simultaneous measurement of temperature, stress, and electric field in GaN HEMTs with micro-Raman spectroscopy. Review of Scientific Instruments, 2017, 88, 113111.	1.3	51
83	Capillary-fed, thin film evaporation devices. Journal of Applied Physics, 2020, 128, .	2.5	51
84	Application of the Kirchhoff Transform to Thermal Spreading Problems With Convection Boundary Conditions. IEEE Transactions on Components, Packaging and Manufacturing Technology, 2014, 4, 408-420.	2.5	47
85	A thermophysical battery for storage-based climate control. Applied Energy, 2017, 189, 31-43.	10.1	47
86	Polymer Infused Porous Surfaces for Robust, Thermally Conductive, Self-Healing Coatings for Dropwise Condensation. ACS Nano, 2020, 14, 14878-14886.	14.6	46
87	Experimental Characterization of the Thermal Time Constants of GaN HEMTs Via Micro-Raman Thermometry. IEEE Transactions on Electron Devices, 2017, 64, 2121-2128.	3.0	45
88	Modeling silica aerogel optical performance by determining its radiative properties. AIP Advances, 2016, 6, .	1.3	44
89	Electrically induced drop detachment and ejection. Physics of Fluids, 2016, 28, .	4.0	44
90	Thermodynamic analysis and optimization of adsorption-based atmospheric water harvesting. International Journal of Heat and Mass Transfer, 2020, 161, 120253.	4.8	44

#	Article	IF	CITATIONS
91	Gravitationally Driven Wicking for Enhanced Condensation Heat Transfer. Langmuir, 2018, 34, 4658-4664.	3.5	42
92	Microscale Liquid Dynamics and the Effect on Macroscale Propagation in Pillar Arrays. Langmuir, 2011, 27, 10360-10364.	3.5	41
93	Wide-Field Magnetic Field and Temperature Imaging Using Nanoscale Quantum Sensors. ACS Applied Materials & Interfaces, 2020, 12, 26525-26533.	8.0	41
94	Thermal transport in suspended silicon membranes measured by laser-induced transient gratings. AIP Advances, 2016, 6, .	1.3	40
95	Threeâ€Tier Hierarchical Structures for Extreme Pool Boiling Heat Transfer Performance. Advanced Materials, 2022, 34, .	21.0	38
96	Zeolite Y adsorbents with high vapor uptake capacity and robust cycling stability for potential applications in advanced adsorption heat pumps. Microporous and Mesoporous Materials, 2015, 201, 151-159.	4.4	36
97	High Heat Flux Evaporation of Low Surface Tension Liquids from Nanoporous Membranes. ACS Applied Materials & Interfaces, 2020, 12, 7232-7238.	8.0	36
98	Microtube Surfaces for the Simultaneous Enhancement of Efficiency and Critical Heat Flux during Pool Boiling. ACS Applied Materials & Interfaces, 2021, 13, 12629-12635.	8.0	36
99	Jumping Droplets Push the Boundaries of Condensation Heat Transfer. Joule, 2018, 2, 205-207.	24.0	35
100	Salt rejection in flow-between capacitive deionization devices. Desalination, 2018, 437, 154-163.	8.2	35
101	High temperature stability of transparent silica aerogels for solar thermal applications. APL Materials, 2019, 7, .	5.1	30
102	Multilayer liquid spreading on superhydrophilic nanostructured surfaces. Applied Physics Letters, 2009, 94, .	3.3	29
103	Numerical investigation of liquid flow with phase change nanoparticles in microchannels. International Journal of Heat and Fluid Flow, 2012, 38, 159-167.	2.4	29
104	Thermal pulse energy harvesting. Energy, 2013, 57, 632-640.	8.8	29
105	Dynamic Evolution of the Evaporating Liquid–Vapor Interface in Micropillar Arrays. Langmuir, 2016, 32, 519-526.	3.5	29
106	Multiscale Dynamic Growth and Energy Transport of Droplets during Condensation. Langmuir, 2018, 34, 9085-9095.	3.5	29
107	Suppressing high-frequency temperature oscillations in microchannels with surface structures. Applied Physics Letters, 2017, 110, .	3.3	28
108	Optimization and thermal characterization of uniform silicon micropillar based evaporators. International Journal of Heat and Mass Transfer, 2018, 127, 51-60.	4.8	28

#	Article	IF	CITATIONS
109	Theoretical and experimental investigation of haze in transparent aerogels. Optics Express, 2019, 27, A39.	3.4	27
110	Size distribution theory for jumping-droplet condensation. Applied Physics Letters, 2019, 114, .	3.3	27
111	Focusing of phase change microparticles for local heat transfer enhancement in laminar flows. International Journal of Heat and Mass Transfer, 2013, 56, 380-389.	4.8	26
112	Spectral splitting optimization for high-efficiency solar photovoltaic and thermal power generation. Applied Physics Letters, 2016, 109, .	3.3	25
113	Simultaneous prediction of dryout heat flux and local temperature for thin film evaporation in micropillar wicks. International Journal of Heat and Mass Transfer, 2019, 136, 170-177.	4.8	25
114	Coexistence of Pinning and Moving on a Contact Line. Langmuir, 2017, 33, 8970-8975.	3.5	24
115	Theory of Thermal Time Constants in GaN High-Electron-Mobility Transistors. IEEE Transactions on Components, Packaging and Manufacturing Technology, 2018, 8, 606-620.	2.5	22
116	Boiling crisis due to bubble interactions. International Journal of Heat and Mass Transfer, 2022, 182, 121904.	4.8	22
117	Droplet mixing using electrically tunable superhydrophobic nanostructured surfaces. Microfluidics and Nanofluidics, 2009, 7, 137-140.	2.2	21
118	Dimensionality effects of carbon-based thermal additives for microporous adsorbents. Materials and Design, 2015, 85, 520-526.	7.0	21
119	Jumping Droplet Electrostatic Charging and Effect on Vapor Drag. Journal of Heat Transfer, 2014, 136, .	2.1	20
120	Framework water capacity and infiltration pressure of MFI zeolites. Microporous and Mesoporous Materials, 2014, 190, 84-91.	4.4	20
121	Radiative Thermal Runaway Due to Negative-Differential Thermal Emission Across a Solid-Solid Phase Transition. Physical Review Applied, 2018, 10, .	3.8	20
122	Understanding triggering mechanisms for critical heat flux in pool boiling based on direct numerical simulations. International Journal of Heat and Mass Transfer, 2020, 163, 120546.	4.8	20
123	The potential for atmospheric water harvesting to accelerate household access to safe water. Lancet Planetary Health, The, 2020, 4, e91-e92.	11.4	20
124	Electrowetting-on-dielectric actuation of a vertical translation and angular manipulation stage. Applied Physics Letters, 2016, 109, .	3.3	18
125	Embedded Microjets for Thermal Management of High Power-Density Electronic Devices. IEEE Transactions on Components, Packaging and Manufacturing Technology, 2019, 9, 269-278.	2.5	18
126	Effects of airborne hydrocarbon adsorption on pool boiling heat transfer. Applied Physics Letters, 2020, 116, .	3.3	18

#	Article	IF	CITATIONS
127	Solarâ€Driven Soft Robots. Advanced Science, 2021, 8, 2004235.	11.2	17
128	Response to Comment on "Water harvesting from air with metal-organic frameworks powered by natural sunlight― Science, 2017, 358, .	12.6	16
129	Athermal operation of multi-section slotted tunable lasers. Optics Express, 2017, 25, 14414.	3.4	16
130	A unified relationship between bubble departure frequency and diameter during saturated nucleate pool boiling. International Journal of Heat and Mass Transfer, 2021, 165, 120640.	4.8	16
131	Unified descriptor for enhanced critical heat flux during pool boiling of hemi-wicking surfaces. International Journal of Heat and Mass Transfer, 2022, 183, 122189.	4.8	16
132	Enhancement of Boiling with Scalable Sandblasted Surfaces. ACS Applied Materials & Interfaces, 2022, 14, 9788-9794.	8.0	16
133	Bubble nucleation, growth, and departure: A new, dynamic understanding. International Journal of Heat and Mass Transfer, 2019, 145, 118803.	4.8	15
134	Transport-Based Modeling of Bubble Nucleation on Gas Evolving Electrodes. Langmuir, 2020, 36, 15112-15118.	3.5	15
135	Heat transfer suppression by suspended droplets on microstructured surfaces. Applied Physics Letters, 2020, 116, .	3.3	15
136	Toward Optimal Heat Transfer of 2D–3D Heterostructures <i>via</i> van der Waals Binding Effects. ACS Applied Materials & Interfaces, 2021, 13, 46055-46064.	8.0	15
137	A hybrid method for bubble geometry reconstruction in two-phase microchannels. Experiments in Fluids, 2006, 40, 847-858.	2.4	14
138	Three-dimensional graphene enhanced heat conduction of porous crystals. Journal of Porous Materials, 2016, 23, 1647-1652.	2.6	14
139	Heat and mass transfer in hygroscopic hydrogels. International Journal of Heat and Mass Transfer, 2022, 195, 123103.	4.8	14
140	Nucleation Site Distribution Probed by Phase-Enhanced Environmental Scanning Electron Microscopy. Cell Reports Physical Science, 2020, 1, 100262.	5.6	13
141	How Coalescing Bubbles Depart from a Wall. Langmuir, 2022, 38, 4371-4377.	3.5	13
142	Enhancement of convective heat transfer in an air-cooled heat exchanger using interdigitated impeller blades. International Journal of Heat and Mass Transfer, 2011, 54, 4549-4559.	4.8	12
143	Electric field dependence of optical phonon frequencies in wurtzite GaN observed in GaN high electron mobility transistors. Journal of Applied Physics, 2016, 120, .	2.5	12
144	Characterization of thin film evaporation in micropillar wicks using micro-Raman spectroscopy. Applied Physics Letters, 2018, 113, .	3.3	12

#	Article	IF	CITATIONS
145	Revisiting the Schrage Equation for Kinetically Limited Evaporation and Condensation. Journal of Heat Transfer, 2022, 144, .	2.1	12
146	Enhanced water transport and salt rejection through hydrophobic zeolite pores. Nanotechnology, 2017, 28, 505703.	2.6	11
147	Hotspot Thermal Management via Thin-Film Evaporation—Part I: Experimental Characterization. IEEE Transactions on Components, Packaging and Manufacturing Technology, 2018, 8, 88-98.	2.5	11
148	Enhanced Environmental Scanning Electron Microscopy Using Phase Reconstruction and Its Application in Condensation. ACS Nano, 2019, 13, 1953-1960.	14.6	11
149	Design of a Microbreather for Two-Phase Microchannel Heat Sinks. Nanoscale and Microscale Thermophysical Engineering, 2009, 13, 151-164.	2.6	10
150	Contributed Review: Experimental characterization of inverse piezoelectric strain in GaN HEMTs via micro-Raman spectroscopy. Review of Scientific Instruments, 2016, 87, 061501.	1.3	10
151	Predicting Surface Tensions of Surfactant Solutions from Statistical Mechanics. Langmuir, 2018, 34, 2386-2395.	3.5	10
152	Temporal Evolution of Surface Contamination under Ultra-high Vacuum. Langmuir, 2022, 38, 1252-1258.	3.5	10
153	Turning traditionally nonwetting surfaces wetting for even ultra-high surface energy liquids. Proceedings of the National Academy of Sciences of the United States of America, 2022, 119, .	7.1	10
154	Alteration of pool boiling heat transfer on metallic surfaces by in situ oxidation. International Journal of Heat and Mass Transfer, 2022, 185, 122320.	4.8	10
155	Controlled Wetting in Nanoporous Membranes for Thin Film Evaporation. Journal of Heat Transfer, 2016, 138, .	2.1	9
156	Transient thermal dynamics of GaN HEMTs. , 2016, , .		9
157	Jumping droplet condensation in internal convective vapor flow. International Journal of Heat and Mass Transfer, 2020, 163, 120398.	4.8	9
158	Criteria for antibubble formation from drop pairs impinging on a free surface. Physical Review Fluids, 2020, 5, .	2.5	9
159	Experiments on the ultrathin silicon vapor chamber for enhanced heat transfer performance. , 2016, , .		8
160	Specular side reflectors for high efficiency thermal-to-optical energy conversion. Optics Express, 2018, 26, A462.	3.4	8
161	Experimental characterization of Si micropillar based evaporator for advanced vapor chambers. , 2014, , , \cdot		7
162	Combined selective emitter and filter for high performance incandescent lighting. Applied Physics Letters, 2017, 111, .	3.3	7

#	Article	IF	CITATIONS
163	Hotspot Thermal Management via Thin-Film Evaporation—Part II: Modeling. IEEE Transactions on Components, Packaging and Manufacturing Technology, 2018, 8, 99-112.	2.5	7
164	Stefan flow induced natural convection suppression on high-flux evaporators. International Communications in Heat and Mass Transfer, 2020, 110, 104255.	5.6	7
165	Framework for analyzing the thermoreflectance spectra of metal thermal transducers with spectrally tunable time-domain thermoreflectance. Journal of Applied Physics, 2020, 128, 055107.	2.5	7
166	Experiment and modeling of microstructured capillary wicks for thermal management of electronics. , 2013, , .		6
167	One-pot solvothermal synthesis of a well-ordered layered sodium aluminoalcoholate complex: a useful precursor for the preparation of porous Al ₂ O ₃ particles. CrystEngComm, 2014, 16, 2950-2958.	2.6	6
168	Ultrathin planar hematite film for solar photoelectrochemical water splitting. Optics Express, 2015, 23, A1491.	3.4	6
169	Bottom-Up Synthesized All-Thermal-Catalyst Aerogels for Heat-Regenerative Air Filtration. Nano Letters, 2021, 21, 8160-8165.	9.1	6
170	Zinc sulfide-pigmented polyethylene aerogel covers for daytime radiative cooling. Journal of Photonics for Energy, 2021, 11, .	1.3	6
171	In-situ aging microwave heating synthesis of LTA zeolite layer on mesoporous TiO2 coated porous alumina support. Journal of Crystal Growth, 2015, 432, 123-128.	1.5	5
172	Response to Comment on "Water harvesting from air with metal-organic frameworks powered by natural sunlight― Science, 2017, 358, .	12.6	5
173	Active fume hood sash height monitoring with audible feedback. Energy Reports, 2018, 4, 645-652.	5.1	5
174	Effect of Al2O3 ALD coating on thermal stability of silica aerogel. Journal of Porous Materials, 2022, 29, 193-200.	2.6	4
175	RECENT ADVANCES IN ADSORPTION-BASED HEATING AND COOLING SYSTEMS. Annual Review of Heat Transfer, 2016, 19, 199-239.	1.0	4
176	Rational Fabrication of Nano-to-Microsphere Polycrystalline Opals Using Slope Self-Assembly. Langmuir, 2021, 37, 12568-12576.	3.5	4
177	Numerical validation of the dusty-gas model for binary diffusion in low aspect ratio capillaries. Physics of Fluids, 2021, 33, .	4.0	4
178	Design and modeling of a multiscale porous ceramic heat exchanger for high temperature applications with ultrahigh power density. International Journal of Heat and Mass Transfer, 2022, 194, 122996.	4.8	4
179	Designed Single-Step Synthesis, Structure, and Derivative Textural Properties of Well-Ordered Layered Penta-coordinate Silicon Alcoholate Complexes. Chemistry - A European Journal, 2014, 20, 6315-6323.	3.3	3
180	Optimization and thermal characterization of uniform micropillar based silicon evaporator in		3

advanced vapor chambers. , 2016, , .

3

#	Article	IF	CITATIONS
181	Detailed thermal resistance model for characterization of the overall effective thermal conductivity of a flat heat pipe. , 2016, , .		3
182	Visualization of the Evaporating Liquid-Vapor Interface in Micropillar Arrays. Journal of Heat Transfer, 2016, 138, .	2.1	3
183	Photonic Crystals: Enabling Ideal Selective Solar Absorption with 2D Metallic Dielectric Photonic Crystals (Adv. Mater. 47/2014). Advanced Materials, 2014, 26, 7922-7922.	21.0	2
184	Plasmonic absorption-induced haze suppression in random scattering media. Applied Physics Letters, 2019, 114, .	3.3	2
185	Quasiâ€Newtonian Environmental Scanning Electron Microscopy (QNâ€ESEM) for Monitoring Material Dynamics in Highâ€Pressure Gaseous Environments. Advanced Science, 2020, 7, 2001268.	11.2	2
186	Scaling the performance of an air-cooled loop heat pipe with the addition of modular condensers. , 2012, , .		1
187	Ostwald Ripening During Freezing on Scalable Superhydrophobic Surfaces. Journal of Heat Transfer, 2014, 136, .	2.1	1
188	Thin-film evaporation from micropillar wicks in ambient environment. , 2017, , .		1
189	Corrections to "Design and Modeling of Membrane-Based Evaporative Cooling Devices for Thermal Management of High Heat Fluxes―[Jul 16 1056-1065]. IEEE Transactions on Components, Packaging and Manufacturing Technology, 2019, 9, 1663-1663.	2.5	1
190	Pulsed Evaporative Transient Thermometry on isolated microstructures. , 2011, , .		0
191	Pulsed evaporative transient thermometry for temporally-resolved thermal measurements. International Journal of Heat and Mass Transfer, 2013, 67, 147-152.	4.8	0
192	Design and fabrication of magnetically tunable microstructured surfaces. , 2013, , .		0
193	Nanoengineered devices for solar energy conversion. , 2017, , .		0
194	Charging of miniature flat heat pipes. Heat and Mass Transfer, 2018, 54, 3131-3136.	2.1	0
195	Manipulating Water and Heat with Nanoengineered Surfaces. Women in Engineering and Science, 2020, , 85-99.	0.4	0